ACS Chemical Neuroscience

Anatolian University Libraries Consortium a·n·k·o·s

Subscriber access provided by HACETTEPE UNIVERSITESI KUTUPHANESI

Article

An ortho-Iminoquinone Compound Reacts with Lysine Inhibiting Aggregation while Remodeling Mature Amyloid Fibrils.

Luiza Fernandes, Nathália Moraes, Fernanda Savacini Sagrillo, Augusto V. Magalhães, Marcela Cristina de Moraes, Luciana Romão, Jeffery W. Kelly, Debora Foguel, Neil P. Grimster, and Fernando L Palhano

ACS Chem. Neurosci., **Just Accepted Manuscript** • Publication Date (Web): 20 Apr 2017

ACS Publications

ACS Chemical Neuroscience is published by the American Chemical Society. 1155 Sixteenth Street N.W., Washington, DC 20036

An *ortho*-Iminoquinone Compound Reacts with Lysine Inhibiting Aggregation while Remodeling Mature Amyloid Fibrils.

Luiza Fernandes[‡], Nathalia Moraes[‡], Fernanda S. Sagrillo[§], Augusto V. Magalhães[‡], Marcela C. de Moraes[§], Luciana Romão[#], Jeffery W. Kelly[†], Debora Foguel[‡], Neil P. Grimster[†] and Fernando L. Palhano[‡,*]

[‡]Instituto de Bioquímica Médica Leopoldo de Meis, Programa de Biologia Estrutural, Universidade Federal do Rio de Janeiro, Rio de Janeiro, 21941-590, Brazil.

[†]Departments of Chemistry and Molecular and Experimental Medicine and the Skaggs Institute for Chemical Biology, The Scripps Research Institute, 10550 N. Torrey Pines Road, La Jolla, CA 92037, USA.

[#]Universidade Federal do Rio de Janeiro – Pólo de Xerém, Duque de Caxias, Rio de Janeiro 25245-390, Brazil.

[§]Department of Organic Chemistry, Chemistry Institute, Fluminense Federal University, Niteroi, Rio de Janeiro, 24020-141, Brazil.

ABSTRACT

Protein aggregation is a hallmark of several neurodegenerative diseases, including Alzheimer's and Parkinson's diseases. It has been shown that lysine residues play a key role in the formation of these aggregates. Thus the ability to disrupt aggregate formation by covalently modifying lysine residues could lead to the discovery of therapeutically relevant anti-amyloidogenesis compounds. Herein, we demonstrate that an *ortho*-iminoquinone (IQ) can be utilized to inhibit amyloid aggregation. Using alpha-synuclein and $A\beta_{1\text{-}40}$ as model systems, we observed that IQ was able to react with lysine residues and reduce amyloid aggregation. We also observed that IQ reacts with free amines within the amyloid fibrils preventing their dissociation and seeding capacity.

Keywords: imine, amyloid aggregation, Parkinson's disease, alpha-synuclein, Alzheimer's disease, cross-link.

INTRODUCTION

The aggregation of peptides and proteins, exacerbated by aging, is genetically and pathologically linked to numerous neurodegenerative diseases, including Alzheimer's disease, Parkinson's disease, as well as the systemic amyloidoses[1]. As such, a wide range of normally soluble intrinsically disordered peptides or folded proteins with well-defined structures can form amyloid fibrils, either through mutation or environmental changes[1]. These amyloid fibrils consist of multiple interacting filaments, which are at least two cross-β-sheets thick. To date, a very limited number of therapies exist that can slow the progression of one of the known amyloidoses[2]. Therefore, compounds capable of directly interacting with amyloidogenic proteins and blocking their self-assembly, or possessing the ability to remodel mature amyloid fibrils, may help in addressing this unmet medical need[2]. Two compounds that fulfill these criteria are the molecular tweezers CLR01[3,4] and epigallocatechin-3-gallate (EGCG) (Fig S1) [5-7]. CLR01 binds with high affinity to lysine (Lys) residues of proteins, thereby affecting the aggregation process of a broad range of amyloidogenic proteins[3]. The molecular mechanisms by which EGCG blocks amyloid aggregation are not completely understood; however, some studies point toward hydrophobic binding and Schiff base formation with Lys residues as important features of the mechanism[5,8]. Moreover, Lys residues have been shown to be important in the aggregation of several amyloidogenic proteins[9].

Recently, inspired by the amine oxidase enzymes[10], Largeron and Fleury developed an *o*-iminoquinone (IQ) compound that catalyzes the oxidation of amines to imines under mild conditions[11] (Fig 1). To accomplish this transformation, however, it was necessary to first oxidize IQ itself (step 1, Fig 1). This initial step can occur through aerobic oxidation, but with a very slow rate of reaction (~ seven days)[11]. In contrast, the presence of metal salts, e.g., copper,

enhances the rate of reaction ~50 fold. The authors demonstrated that under these conditions IQ was capable of oxidizing several primary amines to imines, in methanolic solutions[11]. Due to the ability of this transformation to function under polar protic conditions, we reasoned that it may be possible to oxidize the Lys side-chains of proteins under aqueous conditions, thereby generating imines capable of forming inter- or intra-molecular cross-links.

Our data show that IQ blocks the aggregation of alpha-synuclein and remodels mature amyloid fibrils of alpha-synuclein and $A\beta_{1-40}$ into amorphous material. The molecular mechanisms by which IQ affects the aggregation of fibrils is not fully elucidated, but here we demonstrate that these effects are in part dependent of presence of lysine residues within the fibrils. The data presented here open several new possible avenues of investigation in the amyloid field, and the mechanisms described should therefore be considered during the design of amyloid inhibitors to treat these devastating diseases.

RESULTS AND DISCUSSION

To test the activity of IQ on amyloid aggregation, we first utilized the amyloidogenic protein alpha-synuclein (syn) as a model system. The aggregation of syn in Lewy bodies is a typical pathological hallmark of Parkinson's disease. Syn possesses fifteen lysine residues (Fig 2A). Initially, we incubated monomeric syn (70 μM) with agitation in the presence of thioflavin T (ThT), a fluorogenic amyloid probe, and monitored aggregation by the increase in ThT fluorescence intensity as a function of time (Fig 2B). As hypothesized, there is a dose dependent reduction in the rate of syn aggregation in the presence of IQ (Fig 2B). When a ratio of 1:7 or greater (syn:IQ) was used, complete inhibition of syn aggregation was observed. As a positive control EGCG (Fig S1), a well-known inhibitor of syn aggregation[6], was also studied. Here, syn

aggregation was completely inhibited at a ratio of 1:5 syn:EGCG, indicating that EGCG was slightly more effective at preventing aggregation when compared to IQ. It is also important to note that all subsequent experiments with IQ were performed in the presence of zinc (Zn^{2+}). As a control, we observed no difference in the aggregation of syn monomers when incubated in the presence or absence of zinc, over the time course of our experiments (Fig S3). When syn was incubated with IQ at a ratio of 1:5 in the presence of 1mM zinc, we observed increased inhibitory aggregation activity of IQ when compared to the absence of zinc (Fig S3). When a ratio of 1:10 (syn:IQ) was used, IQ efficiently blocked syn aggregation and this inhibition was not further enhanced by the presence of zinc (Fig S3). In other words, zinc is important, but not essential, for catalyzing the reaction between IQ and syn, especially when lower concentrations of IQ are used.

In an effort to further characterize the effects of IQ on syn aggregation, 70 μM syn was incubated in the presence of either IQ or EGCG (1:10 - syn:compound) for 60 h. The samples were then fractionated by high-speed centrifugation to yield soluble (S) and pellet (P) fractions. Each fraction was subsequently treated with 8 M urea, sonicated for 30 min, boiled for 10 min with SDS in order to solubilize any amyloids fibrils present[12], and resolved by SDS-PAGE (Fig 2C and S4). In the absence of compound, the vast majority of the syn (90%) is found in the pellet, consistent with amyloid formation (Fig 2C, lanes 1 and 2; Fig S4), whereas in the presence of EGCG, only soluble species with different masses (monomer, dimer, trimer, etc.) were detected (Fig 2C, lanes 3 and 4; Fig S4). These cross-linked species are believed to derive from Schiff base formation between the lysine of the protein and a quinone intermediate formed via oxidation of EGCG[6]. In the presence of IQ (1:10 syn:IQ), approximately 80% of the syn was found in the soluble fraction, thus demonstrating IQ's ability to retard aggregate formation (Fig

2C, lane 5; Fig S4). It should be noted, however, that syn was also observed in the pelleted material, suggesting only partial inhibition of aggregation (Fig 2C, lane 6; Fig S4).

To gain further insights into the species formed during aggregation in the presence of IQ, a filter retardation assay (FRA) was employed (Fig 2D). Briefly, syn was incubated for 60 h in the absence or presence of IQ, and then an aliquot of each was boiled with 2% SDS and applied to a membrane (0.2 μm pores), which allows the passage of soluble proteins, but traps larger aggregated species. As expected, the sample incubated in the absence of IQ passed through the membrane, because the aggregates formed in the incubation had been denatured through boiling (Fig 2D). In contrast, when syn was incubated with IQ, part of the sample was retained in the membrane. This suggests a degree of intermolecular cross-linking amongst the fibrils which renders them stable to boiling with SDS (Fig 2D). It is important to note that in our FRA protocol the membrane was stained with Ponceau S, the sensitivity of which is far less than some other detection methods, e.g., immune detection. This may, therefore, explain why we observed no retained fibrils after SDS boiling while others have observed some SDS resistant fibrils[13]. To study the secondary structure of the species formed during aggregation in the presence of IQ, circular dichroism (CD) was employed. In the absence of IQ, syn aggregates displayed the well documented β-sheet secondary structure. In contrast, a random-coil pattern, typical of syn monomers, was observed when aggregation was performed in the presence of IQ (Fig 2E).

Finally, the seeding capacity of fibrils formed in the presence of IQ was investigated. As has been previously demonstrated, fragments of the aggregates formed in the presence of EGCG do not seed the formation of other aggregates ([6] and Fig 2F, green). In contrast, syn fibrils formed in the absence of any compound do seed aggregation (Fig 2F, black). Interestingly, sonication of the aggregates formed in the presence of IQ displayed reduced seeding capacity (Fig 2F -

compare blue with black curve). Collectively, these data suggest that IQ was able to reduce amyloid aggregation of syn, resulting in soluble and insoluble species, and generating some SDS-resistant aggregates with reduced seeding competence.

In order to demonstrate that the effect of IQ on syn aggregation originates from the Lys residues, aggregation assays were performed in the presence and absence of free lysine (Fig 3A). Interestingly, when free lysine (150:1, Lys:IQ) was added to the aggregation of syn in the presence of IQ, the ability of IQ to inhibit aggregation was almost completely blocked. This result suggests that, at least in part, IQ exerts its effect on syn aggregation through reaction with the lysine side chains. TEM analysis of the morphology of the syn aggregates formed in the absence or presence of IQ demonstrated mature fibrils when aggregation was performed in the absence of IQ (Fig. 3B), while amorphous, spherical aggregates were observed in the presence of IQ (1:5, Fig. 3C). Interestingly, the typical fibril architecture was restored when free Lys was present (Fig. 3D). The presence of free Lys also reduced the amount of SDS-resistant aggregates produced upon addition of IQ (Fig 3E).

In order to analyze whether IQ chemically modified syn, monomeric syn was incubated for 60 h under aggregating conditions and subsequently analyzed by mass spectrometry (Fig 3F-I). In the absence of IQ, a single peak corresponding to unmodified syn was observed (mass observed = 14,460 Da) (Fig 3F). However, when aggregation was performed in the presence of IQ, several additional peaks were detected (Fig 3H and 3I). First, we noted the formation of oxidized syn, with masses equivalent to the addition of one (+16), two (+32) or three (+48) oxygens. We also observed the presence of masses corresponding to the addition of one (+164) or two (+328) IQ molecules. Additional peaks for the oxidation (1-3 oxygens) of these adducts were also observed. This analysis also confirmed that Zn^{2+} is important for the catalytic activity of IQ, since all peaks

related to the adduct IQ:syn were less intense in its absence (compare Fig 3H with Fig 3I). Also, Zn^{2+} alone caused no changes in the primary structure of syn (compare Fig 3F with 3G). Moreover, free Lys blocked the formation of the IQ:syn adduct, while the oxidation of syn was still observed (data not shown). It should be noted that fully oxidized syn cannot aggregate[14]. Taken together, these data suggest that part of IQ's ability to prevent syn aggregation is due to oxidation of the monomers (Fig 1A and Fig 3A) and part to the Lys adducts formed upon reaction with IQ.

Next, we were interested in evaluating the ability of IQ to remodel mature fibrils, as has been reported for EGCG[5,8]. To this end, mature amyloid fibrils of syn were produced (see Fig S5 for fibril characterization), and subsequently incubated with IQ (1:20) or EGCG (1:20). It is important to note that EGCG displaces ThT from amyloid fibrils[5] and this explains the reduction in ThT florescence at time point 0 (Fig 4A). This effect was not observed upon incubation with IQ when fibrils of syn (Fig 4A) or fibrils of $A\beta_{1-40}$ (data not shown) were used. As can be seen in Fig 4A, a marked reduction in ThT fluorescence after 24 h was observed for both EGCG and IQ. The remodeling activity displayed by IQ was analyzed by filter retardation assay (Fig 4B). We observed that amyloid fibrils incubated in the presence of either compound became increasingly resistant to SDS/boiling over time (Fig 4B). While the EGCG fibril cross-linking was faster when compared with IQ (Fig 4B), we confirmed IQ's remodeling of mature amyloid fibrils by electron microscopy analysis (compare Fig 4C with Fig 4D) and also their reduced seeding capacity (Fig 4G). We also observed that after incubation with IQ or EGCG the syn fibrils were largely no longer recognized by the conformation-dependent antibody LOC (Fig 4F), an antibody raised against mature amyloid fibrils[15,16]. Consistent with our hypothesis that IQ remodels amyloid fibrils through interaction with Lys residues, we observed that IQ was

ineffective at remodeling syn fibrils when the Lys side chains were blocked by vitamin B6 or acetylation (Fig 5A), or in the presence of excess of free Lys (Fig 5B,5C). We, therefore, concluded that IQ was able to remodel mature amyloid fibrils of syn into SDS-resistant amorphous aggregates that were also seeding incompetent.

In order to determine whether IQ was also effective at remodeling other amyloid fibrils, we examined its effect on the aggregation of $A\beta_{1-40}$ (Fig 6A), a peptide associated with Alzheimer's disease. The $A\beta_{1-40}$ peptide was agitated for 6 d at 37 °C and the resulting amyloid fibrils were characterized by ThT binding (Fig S6A), transmission electron microscopy (Fig S6B), and CD spectroscopy (Fig S6C). We incubated $A\beta_{1-40}$ mature fibrils with IQ (1:20) for 24 h and the remodeling activity was analyzed by the filter retardation assay and ThT binding. The formation of SDS-resistant aggregates (Fig 6B) and the reduction in ThT fluorescence (Fig 6C) in the presence of IQ demonstrate that IQ also efficiently remodels mature $A\beta_{1-40}$ amyloid fibrils.

We next wanted to investigate whether IQ or EGCG could remodel fibrils that lack lysine residues. To investigate this we used mature amyloid fibrils from islet amyloid polypeptide (IAPP), which lacks both Lys and methionine residues, and was synthesized with an acetylated N-terminus (Fig 7A and Fig S7)[5,17]. When IAPP fibrils were incubated with either IQ or EGCG, neither compound was able to cross-link the mature fibrils (Fig 7B), but EGCG was effective in remodeling them, whereas IQ was not (Fig 7C). This result suggests that IQ activity is completely dependent on the presence of free amines, and/or methionines, whereas EGCG is not.

The cytotoxicity of IQ was probed using human embryonic kidney cells (HEK293) (Fig S8). Unlike EGCG, which was highly toxic to these cells in culture, IQ was innocuous up to 500 μM. In order to study the toxicity of IQ in a more physiologically relevant context, we cultured primary murine dopaminergic neurons, the cells that degenerate in Parkinson's disease patients[18].

These neuronal cells, which express the enzyme tyrosine hydroxylase, a marker for dopaminergic neurons[19] (Fig 8A), were incubated for 24 h with increasing concentrations of IQ or EGCG in the presence of 100 μM zinc. EGCG was much more toxic when compared with IQ in neuronal cells (Fig 8B), as observed for HEK293 cells (Fig S8). Neuronal cells were less robust than HEK cells, with the combination of IQ + zinc displaying some toxicity at 200 μM IQ but more pronounced at 500 μM IQ (compare Fig 8B with S8). The reduced cellular toxicity of IQ represents an important advantage of IQ over EGCG in terms of its future use as an anti-amyloidogenic compound.

Finally, the specificity of IQ was probed using competition assays. We incubated monomeric syn in the presence of chicken egg albumin or egg-white lysozyme and analyzed the ability of IQ to inhibit syn aggregation as well as the enzymatic activity of lysozyme. For the competition experiments we used an equimolar concentration of lysines per protein. We observed that the presence of albumin had no effect on syn aggregation, however the presence of lysozyme changed the kinetics of syn aggregation, reducing the lag time (Fig 9A). When the same experiment was performed in the presence of IQ (1:10, syn:IQ), IQ completely blocked syn aggregation even when albumin or lysozyme were present (Fig 9A). These data were confirmed by fractionation of samples followed by SDS-PAGE (Fig 9B), where it is evident that the samples incubated with albumin or lysozyme exhibit the same profile when compared to the sample incubated in the absence of these proteins, even when IQ was present. In order to evaluate the enzymatic activity of lysozyme after IQ treatment, syn was incubated in the presence or absence of lysozyme with or without IQ (1:10, syn:IQ) for 40 h and then added to a culture of *Micrococcus luteus*, a known target of lysozyme[20]. Lysozyme hydrolyzes the beta-glycosidic linkage between N-acetylmuramic acid and N-acetyl glucosamine in the

peptidoglycan of bacterial cell walls. Dead cells were quantified by labeling with an ethidium homodimer probe (Fig 9C)[20]. We observed that the activity of lysozyme was the same in the absence or in the presence of IQ (Fig 9D, Fig S9). With these experiments we conclude that IQ prefers syn to lysozyme, suggesting some specificity. We speculate that the preference of IQ for syn over lysozyme can be explained by the fact that syn is an intrinsically disordered protein (IDP) with more lysines exposed to facilitate IQ attack.

For transthyretin related amyloidoses, a regulatory agency approved drug, tafamidis, is approved to slow disease progression. Tafamidis is a small molecule that binds with high affinity and specificity to the folded protein transthyretin, kinetically stabilizing the tetramer and preventing protein aggregation[21]. Tafamidis is one of the few compounds that specifically inhibits one amyloid disease, owing to the fact that it binds to a natively folded protein. For IDPs such as syn and Aβ, the development of a specific drug is more challenging[2]. IDPs expose more of their residues to the solvent compared to folded proteins which can be taken advantage of to achieve selectivity.

CONCLUSIONS

In conclusion, we believe that IQ can efficiently block amyloid aggregation and remodel mature amyloid fibrils. The mechanism by which IQ operates is not totally elucidated; however, the majority of its action appears to operate through reaction with free amines (Lys) present in the protein/peptide target. It is still unclear if the IQ effect is mediated only by protein biding (Fig 1 step 4; Fig 3H and 3I) or also involves fibril crosslinking (Fig 1, step 6; Fig 4B and Fig 5). We are currently attempting to elucidate which of the syn lysine residues are susceptible to IQ reaction. We believe that the findings presented in this study can be utilized as starting points for

medicinal chemistry efforts towards the development of compounds capable of reducing the aggregation of amyloidogenic proteins or crosslinking amyloid to reduce dissociation-associated proteotoxicity.

EXPERIMENTAL METHODS

IQ synthesis

The IQ synthesis was performed as described previously, with some modifications[22]. Briefly, in a dry 500 mL flask, polyphosphoric acid (110 g) was heated to about 50 °C. When it became less sticky, acetic acid (0.46 g, 7.7 mmol) and 2-nitroresorcinol (1.00 g, 6.5 mmol) were added and the mixture was stirred for 2 h at 70-80 °C. The reaction was quenched by addition of cold water (300 mL) and the reaction mixture was extracted with ethyl acetate (5 x 100 mL). The combined organic layers were dried over anhydrous $MgSO_4$ and the solvent was removed under reduced pressure at 35 °C. Purification of the crude product was performed by column chromatography (silica gel, hexane/EtOAc) affording the pure 1-(3-Amino-2,4-dihydroxyphenyl)-1-ethanone in 72 % yield (0,92 g, 4.7 mmol). This compound (1.0 g, 5.0 mmol) was poured into the hydrogenation flask, followed by the addition of Pt/C (0.1 g, 10 mol %), and the mixture was subjected to hydrogenation at 28 atm (420 psi) at 50 ºC[23]. The reaction was monitored by TLC until total conversion of the starting material was achieved. The catalyst was separated by filtration, and the solvent was removed under vacuum. *o*-Iminoquinone (0.8 g, 4.78 mmol, 95 %) was obtained as a pale yellow solid of suitable purity for further use: mp 209-211 °C; ^{1}H NMR (500 MHz, DMSO-d6) δ 7.14 (d, J = 8.8 Hz, 1 H), 6.40 (d, J = 8.8 Hz, 1 H), 2.50 (s, 3 H); ^{13}C NMR (75 MHz, DMSO-d6) δ 204.0, 150.8, 123.8, 120.9, 113.2, 107.5, 26.5; MS (ESI+) m/z 168 $[M + H]^{+}$.

Preparation of alpha-synuclein (syn)

Syn was purified as described previously by acidification treatment with some modifications[24]. To purify syn monomers, the lyophilized syn was resuspended in water immediately before each experiment, filtered through a 0.22 μm filter and then centrifuged through a Centricon with a 100 kDa cut-off. The homogeneity of monomers was analyzed by analytical size-exclusion chromatography performed using a Superose^{TM}6 10/300 GL column equilibrated with phosphate saline buffer (Fig S2A). Chromatograms were obtained by injecting samples of 10 μL at a 0.5 mL/min flow rate. Elution was monitored by fluorescence (Ex = 275 nm, Em = 320 nm) and absorbance at 280 nm. We also used dynamic light scattering in order to characterize the purified syn. Dynamic light-scattering (DLS) measurements were performed on a Brookhaven Instruments Corp at 25 °C[25]. The hydrodynamic radium of 4 nm was calculated using the diffusion coefficient and the Stokes–Einstein equation (Fig S2B). The identity of syn was confirmed by mass spectrometry. The mature syn amyloid fibrils were obtained by incubation of monomeric syn (140 μM) in phosphate saline buffer (PBS) pH 7.4 with 0.02% NaN_3 with agitation (rotation at 24 rpm) at 25 °C for 6 d.

Preparation of $A\beta_{1-40}$

$A\beta_{1-40}$ fibrils were prepared as previously described[12]. $A\beta_{1-40}$ was synthesized using a standard Fmoc chemistry strategy for solid phase peptide synthesis. The resulting peptide was purified by reversed phase C18 high-performance liquid chromatography (RP-HPLC) and characterized by matrix-assisted laser desorption ionization mass spectrometry using sinapinic acid as a matrix and nanostructure initiator mass spectrometry (NIMS)-TOF analysis was performed using a VoyagerDE STR TOF (Applied Biosytems, Foster City, CA) mass spectrometer in reflectron

mode. The fibrils were produced after 6 d aggregation at 37 °C in 50 mM phosphate buffer pH 7.4, 150 mM NaCl and 0.02% NaN_3 with agitation (rotation at 24 rpm).

Preparation of Islet Amyloid Polypeptide (IAPP)

$IAPP_{Ac8-37}$ was synthesized with an acetylated N-terminus (Ac) by GenScript. The purity was greater than 95% as analyzed by RP-HPLC and the correct mass was confirmed by electrospray ionization (ESI). Peptide stock solutions were prepared by dissolving a weighed amount of peptide in 8 M guanidine HCl, 50 mM phosphate buffer pH 7.4 to obtain a final concentration of 20 mg/ml. The peptides were sonicated for 1 h and centrifuged (10 min at 16,000 g at 25 °C) to remove insoluble material. The concentration of the stock solutions was determined by Bradford assay. The peptide stock solutions were diluted (~80 fold) in 50 mM phosphate buffer pH 7.4, 150 mM NaCl and 0.02% NaN_3 to a final concentration of 0.25 mg/ml and 0.1 M guanidine HCl. The samples were incubated with agitation (rotation at 24 rpm) at 25 °C for 6 d. The fibrils were centrifuged (16,000 g for 10 min at 4 °C), the supernatant was removed and the pellet was stored at -20 °C until use.

EGCG and IQ preparation

EGCG (Fig S1) obtained from Sigma-Aldrich was prepared in fresh ultra-pure water and aliquots of the stock solution (5 mM) were stored at -20 °C until use. Ten milligrams of IQ was dissolved in 100% DMSO to a final concentration of 300 mM. The stock solution was diluted in ultra pure water to a final concentration of 5 mM and stored protected from light at -20 °C until use.

Thioflavin T (ThT) assay

For kinetics experiments, the samples containing ThT (10 μM) were incubated at 37 °C in a 96-well plate (Costar # 3631) together with Teflon spheres, 0.3 cm diameter. Every 5 min, the plates were shaken for 30 s, and fluorescence (excitation at 450 nm, emission at 477 nm) was monitored using a SpectraMax Paradigm Multi-Mode Microplate Reader. For steady state ThT binding assays, the samples were diluted to 5 μM in PBS pH 7.4 containing 20 μM ThT and incubated at 25 °C for 0.5 h. Binding was monitored using a spectrofluorimeter to measure the fluorescence increase (excitation at 450 nm and fluorescence emission at 470-520 nm) at 25 °C.

Filter retardation (FR) assay

The samples were incubated in the presence of 2% SDS and boiled or not for 10 min, then applied to a nitrocellulose membrane using a DOT blot apparatus under vacuum[26]. For the FR assay, the samples were stained using Ponceau.

Circular dichroism

Circular dichroism (CD) measurements were performed in a Jasco spectropolarimeter using a 0.01 mm path-length quartz cuvette. The buffer used for CD measurements was phosphate saline buffer, pH 7.4. Data were averaged for three scans at a speed of 100 nm/min collected in 0.2 nm steps at 25 °C. The baseline (buffer alone) was subtracted from the corresponding spectra.

Fractionation of aggregates

The samples were fractioned through high-speed centrifugation (16,000 g for 30 min, 15 °C) to yield a soluble and a pellet fraction and then each fraction was treated with 8 M urea, sonicated for 30 min and boiled for 10 min with 2% SDS in order to solubilize any amyloids fibrils present.

Mass spectrometry

The samples were diluted to 7.5 μM in 3% acetonitrile and 0.1% formic acid and loaded onto a Waters Nano Acquity system (Waters, Milford, MA). The sample injection volume was 2.0 μl. Proteins were desalted using a trap column (Waters Symmetry C18 180 μm X 20 mm, 5 μm) and the LC was performed with a linear gradient (0–60%) of acetonitrile containing 0.1% formic acid at a 1.0 μL/min flow. Electrospray tandem mass spectra were recorded using a Q-Tof quadrupole/orthogonal acceleration time-of-flight spectrometer (Waters, Milford, MA) interfaced to the Nano Acquity system capillary chromatograph. The ESI voltage was set at 3500 V, the source temperature was 80 °C, and the cone voltage was 30 V. The instrument control and data acquisition were conducted by a MassLynx data system (Version 4.1, Waters), and experiments were performed by scanning from a mass-to-charge ratio (m/z) of 50–2000 using a scan time of 1 s, applied during the whole chromatographic process. All data were processed manually in MassLynx and the average molecular weight was determined through charge state deconvolution using the Maximum entropy Algorithm (MaxEnt 1, Waters, Milford, MA).

Seeding Experiments.

A monomeric solution of protein (syn = 70 μM) was incubated in the absence or presence of 5% seeds in phosphate saline buffer pH 7.4 with agitation. The seeds were produced by 30 min sonication. The samples containing ThT (10 μM) were incubated at 37 °C in a 96-well plate, and every 5 min the fluorescence (excitation at 450 nm, emission at 477 nm) was monitored.

MTT Metabolic Assay.

Primary cultures of dopaminergic neurons were prepared from the mesencephalon of 14-day-old Swiss Mice embryos (E14), as previously described[27]. Pregnant Swiss mice were anesthetized and decapitated; the brain structures of the 14-day-old embryos were removed and dissociated cells were plated on coverslips treated with poly-L-ornithine (1.5 mg/ml; Sigma-Aldrich) in serum-free neurobasal medium. The cultures were incubated at 37 °C in a humidified 5% CO_2 and 95% air chamber for 7 days. These neuronal cell cultures were assayed by immunocytochemistry with anti-tyrosine hydroxylase (1:100; Millipore) antibody and anti-MAP2 (1:100; Millipore). The cells were incubated with increasing concentrations of IQ or EGCG in the presence of 0.1 M zinc sulfate for 24 h. HEK293 cells were cultured in DMEM medium supplemented with 10% FBS, 100 U/mL gentamicin in a 5% CO_2 humidified environment at 37 °C. Cells were plated at a density of 10,000 cells/well on 96-well plates in 100 µL of fresh medium. After 24 h, the compounds were added, and the cells were incubated for 2 d at 37 °C. Cytotoxicity was measured utilizing the 3-4,5-dimethylthiazolyl-2,5-diphenyltetrazolium bromide (MTT) assay. Absorbance values of formazan were determined at 570 nm after 0.5 h of incubation.

Electron Microscopy

Copper grids (carbon- and formvar-coated 400 mesh) (Electron Microscopy Sciences, Hatfield PA) were glow discharged and 2 µL of sample was applied for 3 min. Excess sample was removed and the grids immediately incubated with 2 % uranyl acetate solution for 2 min. Excess stain was removed and the grid allowed to dry thoroughly. Grids were then examined on a Tecnai Spirit (FEI Company) microscopy at 120 kV.

Chemical blocking of lysines of amyloid fibrils.

Syn amyloid fibrils (120 μM) in 20 mM borate buffer pH 8.0 were incubated with 10 mM acetic anhydride overnight at 25 °C. The acetylated fibrils were dialyzed overnight against phosphate buffer pH 7.4. For pyridoxal 5'-phosphate (PLP) modification, syn amyloid fibrils (120 μM) in 20 mM borate buffer were incubated with 10 mM PLP for 2 h, then 20 mM sodium borohydride was added for 1 h at 25 °C. The PLP-modified fibrils were dialyzed overnight against phosphate buffer pH 7.4. All reactions were performed protected from light.

Dot blot

LOC antibody was raised against mature amyloid fibrils derived from islet amyloid polypeptide. This antibody can distinguish between amyloid fibrils and oligomeric and monomeric species[15]. The samples were spotted (2 μl) onto a nitrocellulose membrane. The membrane was blocked using 1 vol PBS + 1 vol blocking solution (Odyssey) for 1 h. The membrane was incubated with LOC antibody (1:1,000, Millipore) or syn-1 antibody (1:1,000, Sigma) (diluted in 1 vol TBST (50 mM Tris pH 7.6, 0.9% NaCl, 0.1% Tween 20) +1 vol blocking solution for 1 h, washed 3 times with TBST and then incubated for 1 h with goat anti-rabbit secondary antibody conjugated to IRDye 800 CW (1:5,000) for LOC or goat anti-mouse secondary antibody conjugated to IRDye 680 CW (1:5,000) for syn-1 and developed/quantified using an Odyssey Infrared Imaging System.

Competition assay with lysozyme and albumin

Monomeric syn (70 μM) was incubated in the absence or in the presence of 52 μM chicken egg albumin (Uniprot ID: P01012, Sigma) or 175 μM egg-white lysozyme (Uniprot ID: P00698, Sigma) in order to have equimolar concentration of lysines for each protein (1 mM). The samples were incubated at 37 °C in PBS in the absence or in the presence of 700 μM IQ + 1 mM $ZnSO_4$,

as described in the "Thioflavin T (ThT) assay". After 40 h aggregation, an aliquot of the samples was processed as described in the "Fractionation of aggregates". To assess the enzymatic activity of lysozyme, we modified the previous method described by Shugar[28]. *Micrococcus luteus* was grown overnight on Supplemented Tryptic Soy Broth (TSB) under aerobic conditions (200 rpm, 37 °C). The bacteria was centrifuged at 16,000 g 10 °C for 10 min, resuspended in 0.1M potassium phosphate buffer pH 7.0 to give an OD_{450nm}=2.0 and stored at 4 °C. One µl of each sample (syn, syn+IQ, syn+lysozyme or syn+lysozyme+IQ) was incubated with 5 µl cells for 1 h at 25 °C. One micromolar ethidium homodimer (Thermo Fisher) was added and the cells were analyzed in EVOS Cell Imaging Fluorescence Microscopy under 40 X objective.

Data Processing

The error bars represent the S.D. of three independent measurements. For all experiments, the graphics or images presented are representative of three independent experiments.

ASSOCIATED CONTENT

Supporting Information

Additional figures S1 to S9. This material is available free of charge via the Internet at http://pubs.acs.org.

AUTHOR INFORMATION

Corresponding Author

palhano@bioqmed.ufrj.br

AUTHOR CONTRIBUTIONS

FLP and NPG conceived and coordinated the study. LF, NPG, JWK, DF and FLP wrote the paper. LF, NM and FLP designed, performed and analyzed all experiments. NPG, NM, FSS and MCM were responsible by the synthesis and characterization of *ortho*-iminoquinone. LR provided assistance and contributed to the experiments with dopaminergic cells. AVM was responsible for mass spectrometry experiments and analyses.

FUNDING SOURCES

This work was supported by grants from the Conselho Nacional de Desenvolvimento Científico e Tecnológico (CNPq), the Fundação Carlos Chagas Filho de Amparo à Pesquisa do Estado do Rio de Janeiro (FAPERJ) and the Coordenação de Aperfeiçoamento de Pessoal de Nível Superior (CAPES).

CONFLICT OF INTEREST

The authors declare no conflict of interest.

ACKNOWLEDGMENT

We thank Satiago Alonso and Ana Lucia O. Carvalho for technical assistance. We also thank Dr Colleen Fearns for critical reading of the manuscript. We thank Dra Rossolina Zingali for the use of her laboratory facilities. We thank Dr Marco Antônio Miguel for providing the *Micrococcus luteus* strain.

REFERENCES

(1) Chiti, F., and Dobson, C. M. (2006) Protein misfolding, functional amyloid, and human disease. *Annu. Rev. Biochem. 75*, 333–366.

(2) Eisele, Y. S., Monteiro, C., Fearns, C., Encalada, S. E., Wiseman, R. L., Powers, E. T., and Kelly, J. W. (2015) Targeting protein aggregation for the treatment of degenerative diseases. *Nat Rev Drug Discov 14*, 759–780.

(3) Sinha, S., Lopes, D. H. J., Du, Z., Pang, E. S., Shanmugam, A., Lomakin, A., Talbiersky, P., Tennstaedt, A., McDaniel, K., Bakshi, R., Kuo, P.-Y., Ehrmann, M., Benedek, G. B., Loo, J. A., Klärner, F.-G., Schrader, T., Wang, C., and Bitan, G. (2011) Lysine-Specific Molecular Tweezers Are Broad-Spectrum Inhibitors of Assembly and Toxicity of Amyloid Proteins. *J. Am. Chem. Soc. 133*, 16958–16969.

(4) Lump, E., Castellano, L. M., Meier, C., Seeliger, J., Erwin, N., Sperlich, B., Stürzel, C. M., Usmani, S., Hammond, R. M., Einem, von, J., Gerold, G., Kreppel, F., Bravo-Rodriguez, K., Pietschmann, T., Holmes, V. M., Palesch, D., Zirafi, O., Weissman, D., Sowislok, A., Wettig, B., Heid, C., Kirchhoff, F., Weil, T., Klärner, F.-G., Schrader, T., Bitan, G., Sanchez-Garcia, E., Winter, R., Shorter, J., and Münch, J. (2015) A molecular tweezer antagonizes seminal amyloids and HIV infection. *eLife 4*, 10727.

(5) Palhano, F. L., Lee, J., Grimster, N. P., and Kelly, J. W. (2013) Toward the Molecular Mechanism(s) by Which EGCG Treatment Remodels Mature Amyloid Fibrils. *J. Am. Chem. Soc. 135*, 7503–7510.

(6) Ehrnhoefer, D. E., Bieschke, J., Boeddrich, A., Herbst, M., Masino, L., Lurz, R., Engemann, S., Pastore, A., and Wanker, E. E. (2008) EGCG redirects amyloidogenic polypeptides into unstructured, off-pathway oligomers. *Nat. Struct. Mol. Biol 15*, 558–566.

(7) Ehrnhoefer, D. E., Duennwald, M., Markovic, P., Wacker, J. L., Engemann, S., Roark, M., Legleiter, J., Marsh, J. L., Thompson, L. M., Lindquist, S., Muchowski, P. J., and Wanker, E. E. (2006) Green tea (-)-epigallocatechin-gallate modulates early events in huntingtin misfolding and reduces toxicity in Huntington's disease models. *Hum. Mol. Gen 15*, 2743–2751.

(8) Bieschke, J., Russ, J., Friedrich, R. P., Ehrnhoefer, D. E., Wobst, H., Neugebauer, K., and Wanker, E. E. (2010) EGCG remodels mature -synuclein and amyloid- fibrils and reduces cellular toxicity. *Proc Natl Acad Sci USA 107*, 7710–7715.

(9) Sinha, S., Lopes, D. H. J., and Bitan, G. (2012) A Key Role for Lysine Residues in Amyloid β-Protein Folding, Assembly, and Toxicity. *ACS Chem. Neurosci. 3*, 473–481.

(10) Finney, J., Moon, H.-J., Ronnebaum, T., Lantz, M., and Mure, M. (2014) Archives of Biochemistry and Biophysics. *Arch. Biochem. Biophys. 546*, 19–32.

(11) Largeron, M., and Fleury, M.-B. (2012) A Biologically Inspired Cu I/Topaquinone-Like Co-Catalytic System for the Highly Atom-Economical Aerobic Oxidation of Primary Amines to Imines. *Angew. Chem. Int. Ed. 51*, 5409–5412.

(12) Murray, A. N., Palhano, F. L., Bieschke, J., and Kelly, J. W. (2013) Surface adsorption considerations when working with amyloid fibrils in multiwell plates and Eppendorf tubes. *Protein Sci. 22*, 1531–1541.

(13) Lam, H. T., Graber, M. C., Gentry, K. A., and Bieschke, J. (2016) Stabilization of α-Synuclein Fibril Clusters Prevents Fragmentation and Reduces Seeding Activity and Toxicity. *Biochemistry 55*, 675–685.

(14) Hokenson, M. J., Uversky, V. N., Goers, J., Yamin, G., Munishkina, L. A., and Fink, A. L. (2004) Role of individual methionines in the fibrillation of methionine-oxidized alpha-synuclein. *Biochemistry 43*, 4621–4633.

(15) Kayed, R., Head, E., Sarsoza, F., Saing, T., Cotman, C. W., Necula, M., Margol, L., Wu, J., Breydo, L., Thompson, J. L., Rasool, S., Gurlo, T., Butler, P., and Glabe, C. G. (2007) Fibril specific, conformation dependent antibodies recognize a generic epitope common to amyloid fibrils and fibrillar oligomers that is absent in prefibrillar oligomers. *Mol Neurodegener. 2*, 18.

(16) Greiner, E. R., Kelly, J. W., and Palhano, F. L. (2014) Immunoprecipitation of Amyloid Fibrils by the Use of an Antibody that Recognizes a Generic Epitope Common to Amyloid Fibrils. *PLoS ONE 9*, e105433.

(17) Cao, P., and Raleigh, D. P. (2012) Analysis of the Inhibition and Remodeling of Islet Amyloid Polypeptide Amyloid Fibers by Flavanols. *Biochemistry 51*, 2670–2683.

(18) Rodrigues, T. M., Jerónimo-Santos, A., Outeiro, T. F., Sebastião, A. M., and Diógenes, M. J. (2014) Challenges and promises in the development of neurotrophic factor-based therapies for Parkinson's disease. *Drugs Aging 31*, 239–261.

(19) St Martin, J. L., Klucken, J., Outeiro, T. F., Nguyen, P., Keller-McGandy, C., Cantuti-Castelvetri, I., Grammatopoulos, T. N., Standaert, D. G., Hyman, B. T., and McLean, P. J. (2007) Dopaminergic neuron loss and up-regulation of chaperone protein mRNA induced by targeted over-expression of alpha-synuclein in mouse substantia nigra. *J. Neurochem. 100*, 1449–1457.

(20) Dutta, P., Ray, N., Roy, S., Dasgupta, A. K., Bouloussa, O., and Sarkar, A. (2011) Covalent immobilization of active lysozyme on Si/glass surface using alkoxy Fischer carbene complex on SAM. *Org. Biomol. Chem. 9*, 5123–5128.

(21) Bulawa, C. E., Connelly, S., Devit, M., Wang, L., Weigel, C., Fleming, J. A., Packman, J., Powers, E. T., Wiseman, R. L., Foss, T. R., Wilson, I. A., Kelly, J. W., and Labaudiniere, R. (2012) Tafamidis, a potent and selective transthyretin kinetic stabilizer that inhibits the amyloid

cascade. *Proc Natl Acad Sci USA 109*, 9629–9634.

(22) Xu, D., Chiaroni, A., Fleury, M.-B., and Largeron, M. (2006) Electrochemically induced cascade reaction for the assembly of libraries of biologically relevant 1,4-benzoxazine derivatives. *J. Org. Chem. 71*, 6374–6381.

(23) Facchinetti, V., Guimarães, F. A., Souza, M. V. N., Gomes, C. R. B., Souza, M. C. B. V., Wardell, J. L., Wardell, S. M. S. V., and Vasconcelos, T. R. A. (2015) Synthesis of Novel Ethyl (substituted)phenyl□4□oxothiazolidin□3□yl)□1□ethyl□4□oxo□1,4□dihydroquinoline□3□ Carboxylates as Potential Anticancer Agents. *J. Heterocyclic Chem. 52*, 1245–1252.

(24) Coelho-Cerqueira, E., Carmo-Gonçalves, P., Pinheiro, A. S., Cortines, J., and Follmer, C. (2013) α-Synuclein as an intrinsically disordered monomer--fact or artefact? *FEBS J. 280*, 4915–4927.

(25) Dusa, A., Kaylor, J., Edridge, S., Bodner, N., Hong, D.-P., and Fink, A. L. (2006) Characterization of Oligomers during α-Synuclein Aggregation Using Intrinsic Tryptophan Fluorescence. *Biochemistry 45*, 2752–2760.

(26) Wanker, E. E., Scherzinger, E., Heiser, V., Sittler, A., Eickhoff, H., and Lehrach, H. (1999) Membrane filter assay for detection of amyloid-like polyglutamine-containing protein aggregates. *Meth. Enzymol. 309*, 375–386.

(27) Romão, L. F., Sousa, V. de O., Neto, V. M., and Gomes, F. C. A. (2008) Glutamate activates GFAP gene promoter from cultured astrocytes through TGF-beta1 pathways. *J. Neurochem. 106*, 746–756.

(28) Shugar, D. (1952) The measurement of lysozyme activity and the ultra-violet inactivation of lysozyme. *Biochim Biophys Acta 8*, 302–309.

(25) Rodrigues, T. M., Jerónimo-Santos, A., Outeiro, T. F., Sebastião, A. M., and Diógenes, M.

J. (2014) Challenges and promises in the development of neurotrophic factor-based therapies for Parkinson's disease. *Drugs Aging 31*, 239–261.

(26) St Martin, J. L., Klucken, J., Outeiro, T. F., Nguyen, P., Keller-McGandy, C., Cantuti-Castelvetri, I., Grammatopoulos, T. N., Standaert, D. G., Hyman, B. T., and McLean, P. J. (2007) Dopaminergic neuron loss and up-regulation of chaperone protein mRNA induced by targeted over-expression of alpha-synuclein in mouse substantia nigra. *J. Neurochem. 100*, 1449–1457.

(27) Dutta, P., Ray, N., Roy, S., Dasgupta, A. K., Bouloussa, O., and Sarkar, A. (2011) Covalent immobilization of active lysozyme on Si/glass surface using alkoxy Fischer carbene complex on SAM. *Org. Biomol. Chem. 9*, 5123–5128.

(28) Bulawa, C. E., Connelly, S., Devit, M., Wang, L., Weigel, C., Fleming, J. A., Packman, J., Powers, E. T., Wiseman, R. L., Foss, T. R., Wilson, I. A., Kelly, J. W., and Labaudiniere, R. (2012) Tafamidis, a potent and selective transthyretin kinetic stabilizer that inhibits the amyloid cascade. *Proc Natl Acad Sci U S A. 109*, 9629–9634.

FIGURE CAPTIONS

Figure 1. Catalytic oxidation of free amines from lysines into imines by *o*-iminoquinone (IQ).

Figure 2. Effect of IQ on aggregation of syn. (A) Primary sequence of syn. (B) A kinetic experiment of syn (70 μM) aggregation, monitored by ThT fluorescence, was performed in the absence or in the presence of EGCG or IQ. After 60 h aggregation, the samples were: (C) fractionated by centrifugation and resolved by SDS-PAGE, (D) separated using a filter retardation assay and the membrane was stained with Ponceau, and (E) analyzed by Circular dichroism. (F) A monomeric solution of syn (70 μM) was incubated in the absence or presence of 5% seeds. The seeds were produced by sonication of final product of panel B.

Figure 3. IQ acts upon syn aggregation through Lys modification and methionine oxidation. (A) Syn monomers (70 μM) were incubated in the absence or presence of IQ (350 μM) and Lys (50 mM). ThT fluorescence was monitored over time. After aggregation, the morphology of the samples was analyzed by TEM (B, C and D). After 60 h incubation, the samples were analyzed by filter retardation assay (E) and mass spectrometry (F, G, H and I).

Figure 4. IQ remodels mature amyloid fibrils of syn. (A) Mature fibrils of syn (15 μM) were incubated in the absence or in the presence of IQ (300 μM) or EGCG (300 μM) for 0 or 24 h and the ThT fluorescence was measured. (B) A kinetic analysis by filter retardation assay of aliquots of the samples described in panel A. TEM images of samples described in panel A after 24 h

incubation (C, D and E). (F) Dot blot using the LOC antibody that recognizes a generic amyloid epitope. Mature syn fibrils were incubated in the absence or in the presence of IQ or EGCG for 24 h then spotted onto nitrocellulose membrane and then probed with LOC or syn antibody. (G) A monomeric solution of syn (70 μM) was incubated in the absence or presence of 5% seeds. The seeds were produced by sonication of final product of panel A after 24 h incubation.

Figure 5. The amyloid remodeling activity of IQ requires free amines. (A) Syn mature amyloid fibrils were incubated in the presence of pyridoxal 5'-phosphate (VitB6) or acetic aldehyde (AA) in order to block free amines. Chemically modified fibrils (15 μM) were incubated in the absence or presence of IQ (300 μM) for 24 h and aggregation assessed using the FR assay stained with Ponceau. Non-modified fibrils were used as control. (B and C) Mature fibrils of syn (15 μM) were incubated alone, in the presence of IQ (300 μM), or in the presence of IQ (300 μM) and lys (50 mM) for 24 h and aggregation was assessed using (B) the FR assay stained with Ponceau or (C) ThT fluorescence.

Figure 6. IQ remodels mature amyloid fibrils of $A\beta_{1\text{-}40}$. Mature fibrils of $A\beta_{1\text{-}40}$ (A) (15 μM) were incubated in the absence or in the presence of IQ (300 μM) or EGCG (300 μM) for 24 h and remodeling was assessed using (B) the filter retardation assay or (C) ThT fluorescence.

Figure 7. The amyloid remodeling activity of IQ differs from EGCG. (A) $IAPP_{Ac8\text{-}24}$ mature amyloid fibrils (15 μM) were incubated in the absence or presence of IQ (300 μM) or EGCG

(300 μM) for 24 h. An aliquot of these samples was boiled or not in 2% SDS and then applied to FR membrane and stained with Ponceau (B) or ThT fluorescence was measured (C).

Figure 8. Toxicity of IQ and EGCG in murine dopaminergic cells. (A) Primary dopaminergic neurons characterized by the presence of tyrosine hydroxylase and microtubule-associated protein 2 (MAP2) were incubated with 100 μM zinc and different concentrations of IQ or EGCG and after 24 h the viability was measured by MTT assay (B).

Figure 9. IQ blocks the aggregation of syn without affecting the enzymatic activity of lysozyme. (A) A kinetic experiment of syn (70 μM) aggregation, monitored by ThT fluorescence, was performed in the absence or in the presence of 700 μM IQ (1:10). For the competition assay, syn (70 μM) was incubated in the presence of 52 μM chicken egg albumin or 175 μM egg-white lysozyme. After 40 h aggregation, the samples were: (B) fractionated by centrifugation and resolved by SDS-PAGE or (C and D) incubated in the presence of *Micrococcus luteus* to test for the antimicrobial activity of lysozyme. After 1 h incubation, the *Micrococcus luteus* were stained with ethidium homodimer and analyzed by fluorescence microscopy. Bacteria stained red (C) were considered dead bacteria (D).

1 Fig 1

Fig 1

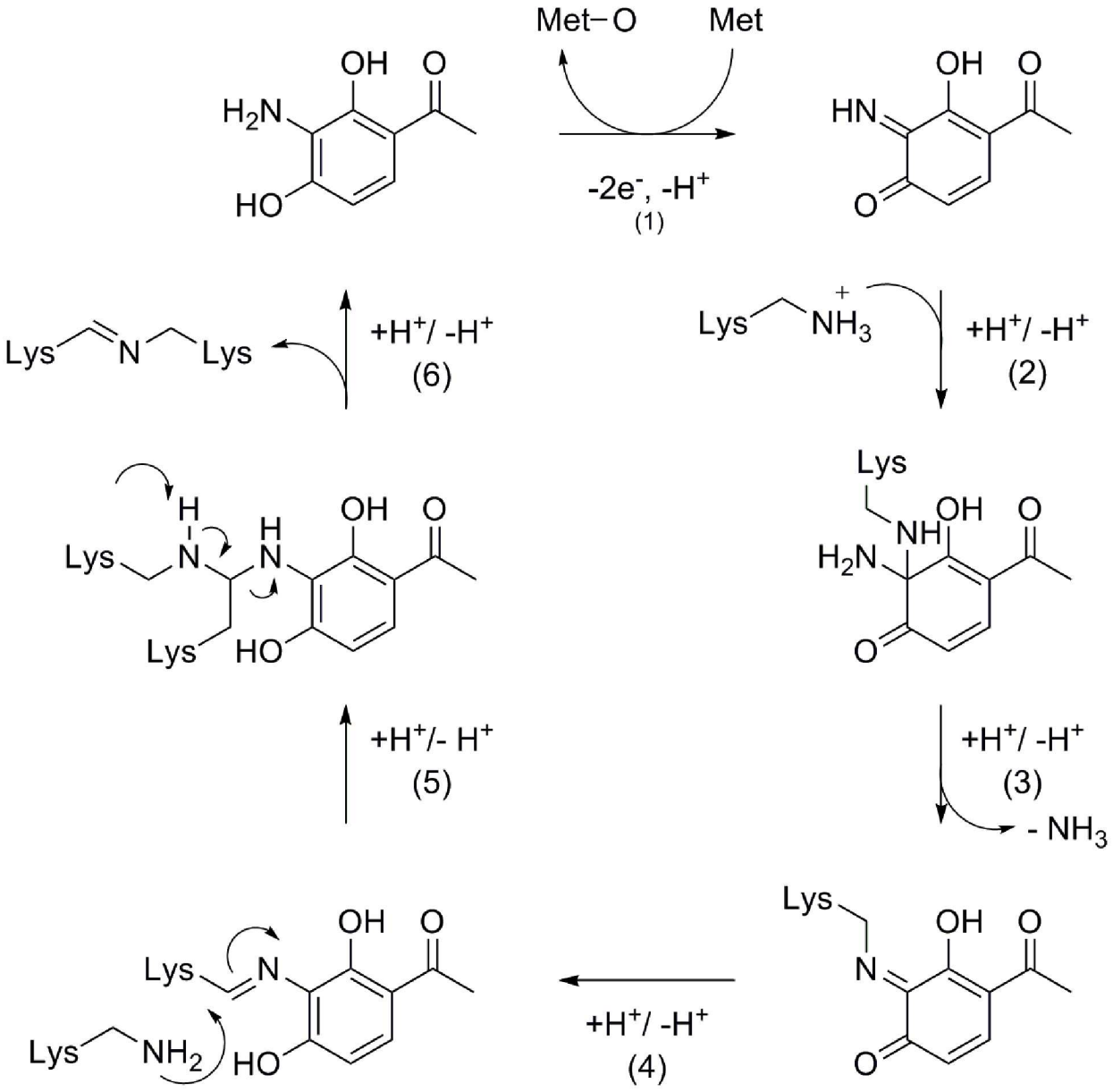

2

3

Fig 2

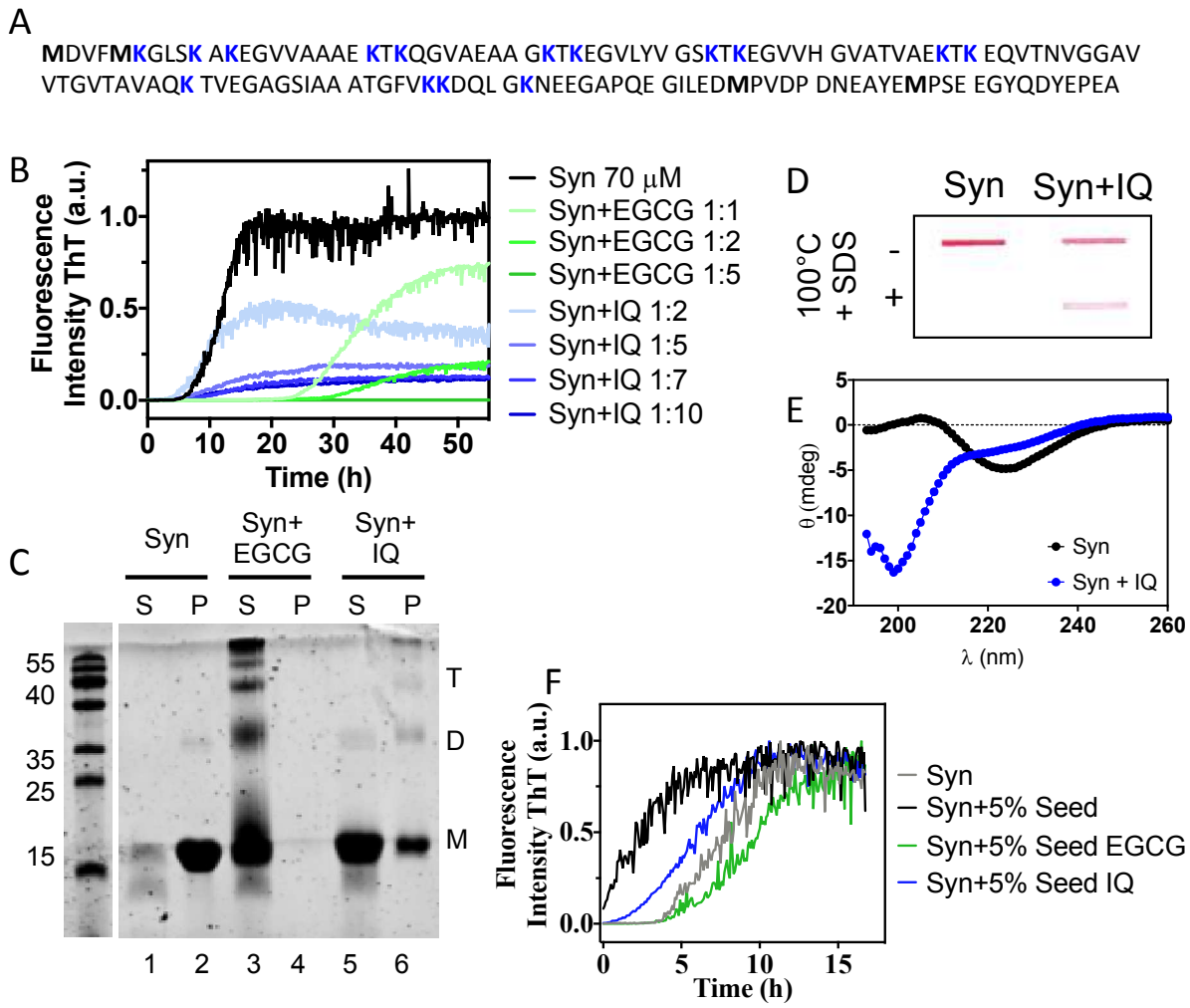
A
MDVFMKGLSK AKEGVVAAAE KTKQGVAEAA GKTKEGVLYV GSKTKEGVVH GVATVAEKTK EQVTNVGGAV
VTGVTAVAQK TVEGAGSIAA ATGFVKKDQL GKNEEGAPQE GILEDMPVDP DNEAYEMPSE EGYQDYEPEA
B
Fluorescence Intensity ThT (a.u.)
Time (h)
Syn 70 μM
Syn+EGCG 1:1
Syn+EGCG 1:2
Syn+EGCG 1:5
Syn+IQ 1:2
Syn+IQ 1:5
Syn+IQ 1:7
Syn+IQ 1:10
C
Syn
Syn+ EGCG
Syn+ IQ
S P S P S P
55
40
35
25
15
T
D
M
1 2 3 4 5 6
D
Syn Syn+IQ
100°C + SDS
-
+
E
θ (mdeg)
λ (nm)
Syn
Syn + IQ
F
Fluorescence Intensity ThT (a.u.)
Time (h)
Syn
Syn+5% Seed
Syn+5% Seed EGCG
Syn+5% Seed IQ

1 Fig 3

Fig 3

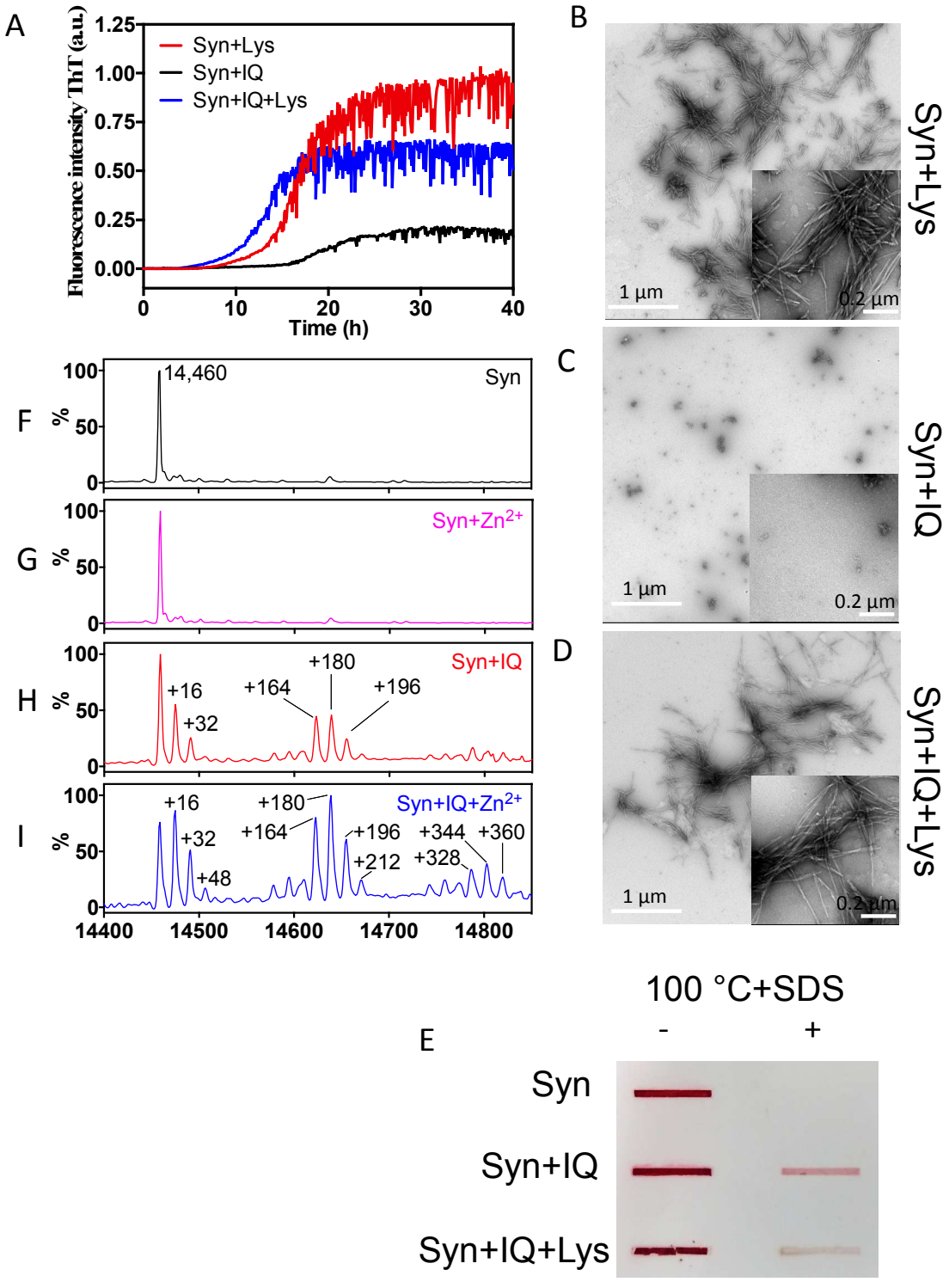
A
Fluorescence intensity ThT (a.u.)
1.25
1.00
0.75
0.50
0.25
0.00
0
10
20
30
40
Time (h)
Syn+Lys
Syn+IQ
Syn+IQ+Lys
B
Syn+Lys
1 µm
0.2 µm
C
Syn+IQ
1 µm
0.2 µm
D
Syn+IQ+Lys
1 µm
0.2 µm
F
Syn
14,460
G
Syn+Zn2+
H
Syn+IQ
+16
+32
+164
+180
+196
I
Syn+IQ+Zn2+
+16
+32
+48
+164
+180
+196
+212
+328
+344
+360
%
100
50
0
14400
14500
14600
14700
14800
E
100 °C+SDS
-
+
Syn
Syn+IQ
Syn+IQ+Lys

2

Fig 4

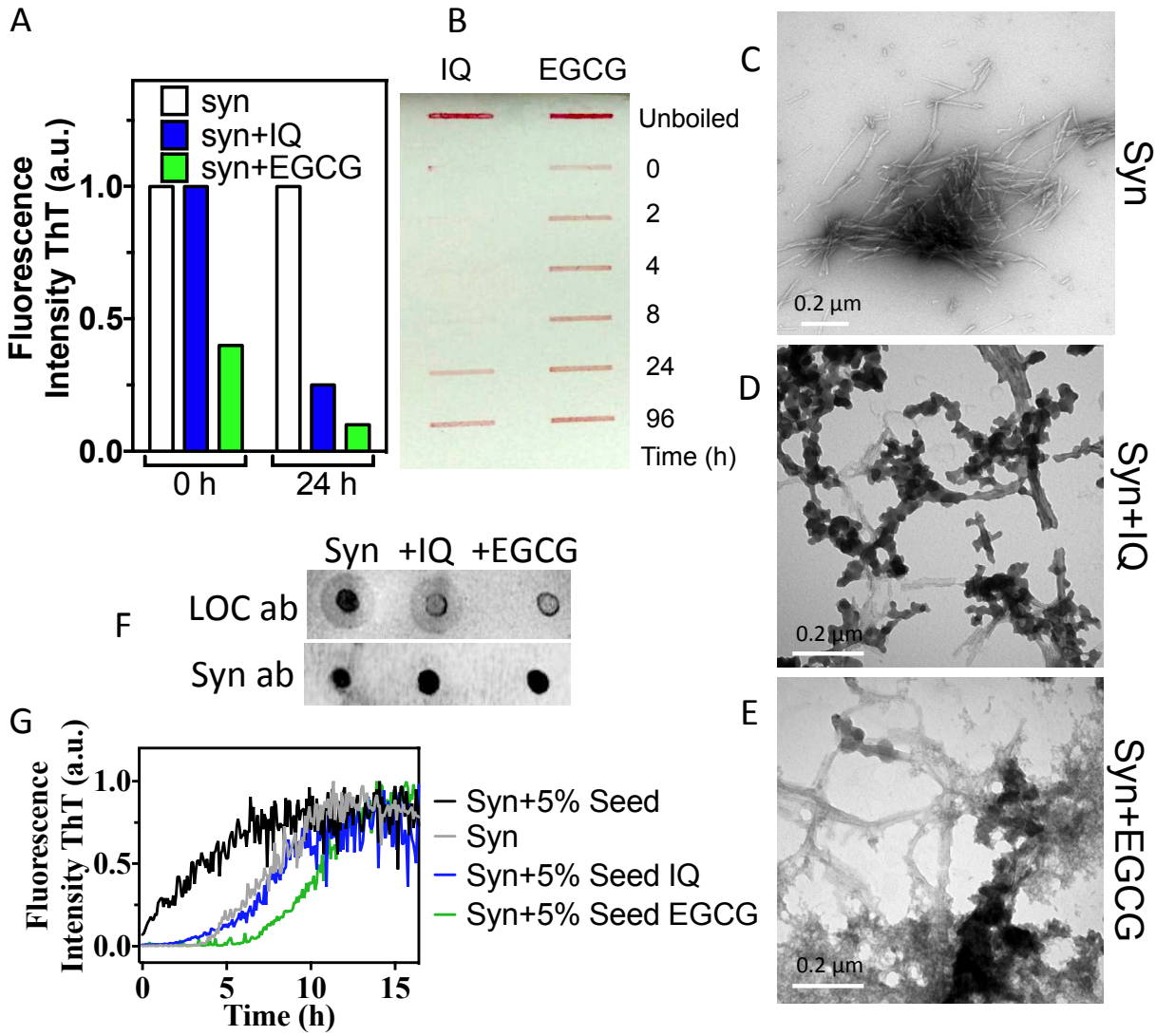
A
B
IQ
EGCG
C
syn
syn+IQ
syn+EGCG
Fluorescence Intensity ThT (a.u.)
1.0
0.5
0.0
0 h
24 h
Unboiled
0
2
4
8
24
96
Time (h)
Syn
0.2 µm
D
Syn+IQ
0.2 µm
E
Syn+EGCG
0.2 µm
Syn +IQ +EGCG
F
LOC ab
Syn ab
G
Fluorescence Intensity ThT (a.u.)
1.0
0.5
0.0
0
5
10
15
Time (h)
Syn+5% Seed
Syn
Syn+5% Seed IQ
Syn+5% Seed EGCG

Fig 5

Fig 5

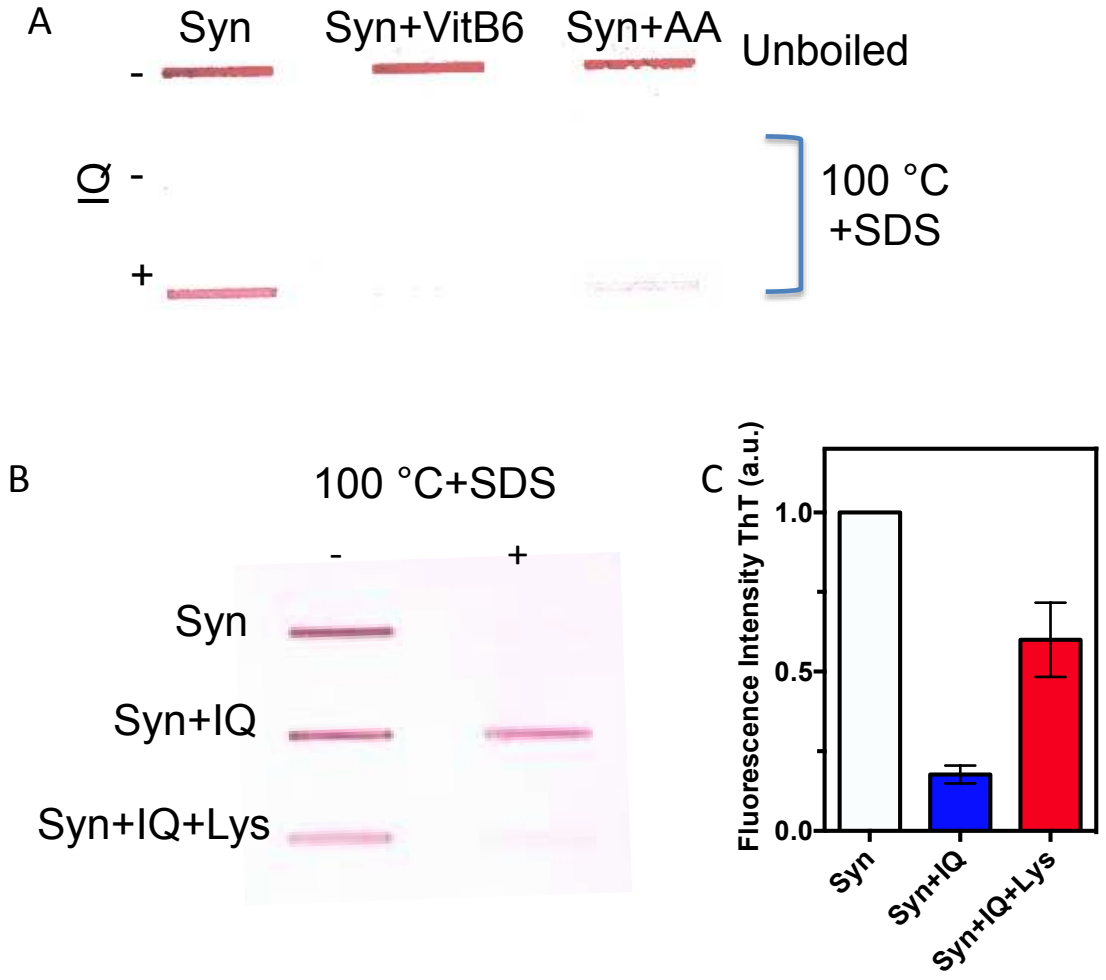
A
Syn
Syn+VitB6
Syn+AA
Unboiled
-
Ø -
+
100 °C
+SDS
B
100 °C+SDS
-
+
Syn
Syn+IQ
Syn+IQ+Lys
C
Fluorescence Intensity ThT (a.u.)
1.0
0.5
0.0
Syn
Syn+IQ
Syn+IQ+Lys

Fig 6

Fig 6

A

$A\beta_{1-40}$DAEFRHDSGYEVHHQKLVFFAE
DVGSNKGAIIGL**M**VGGVV

B

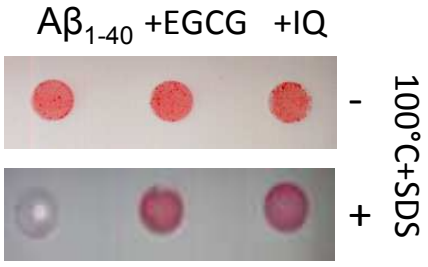

C

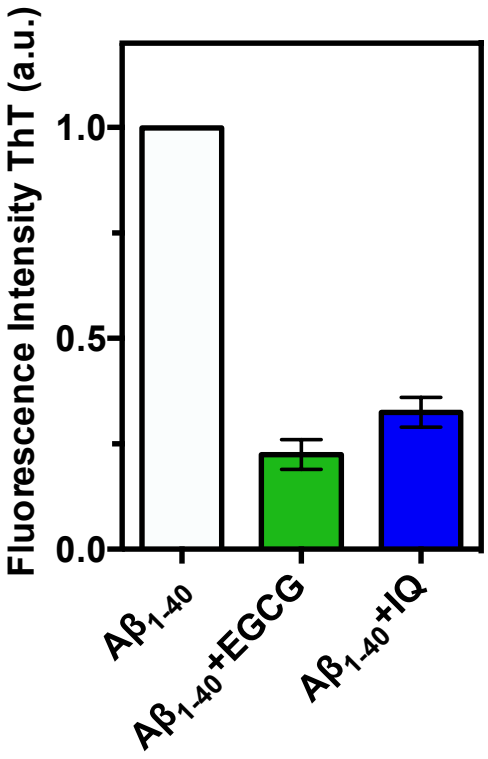

Fig 7

Fig 7

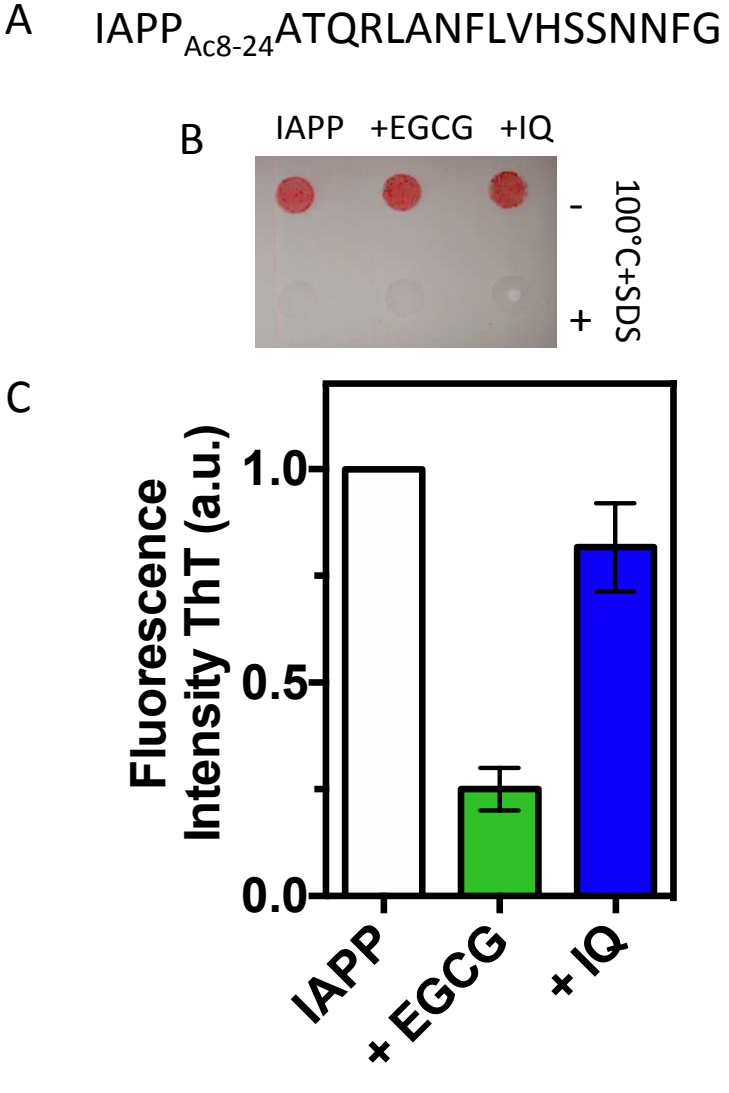
A
IAPP$_{Ac8-24}$ATQRLANFLVHSSNNFG
B
IAPP
+EGCG
+IQ
-
+
100°C+SDS
C
Fluorescence Intensity ThT (a.u.)
1.0
0.5
0.0
IAPP
+ EGCG
+ IQ

Fig 8

Fig 8

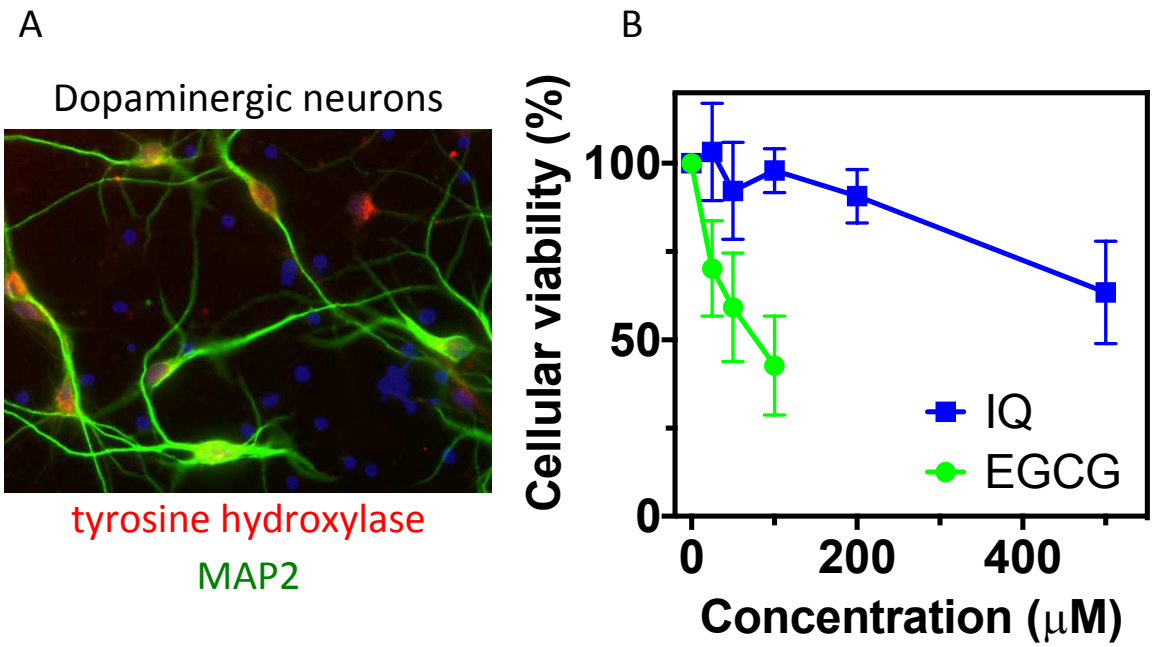
A
Dopaminergic neurons
tyrosine hydroxylase
MAP2
B
Cellular viability (%)
100
50
0
0
200
400
Concentration (μM)
IQ
EGCG

1 Fig 9

Fig 9

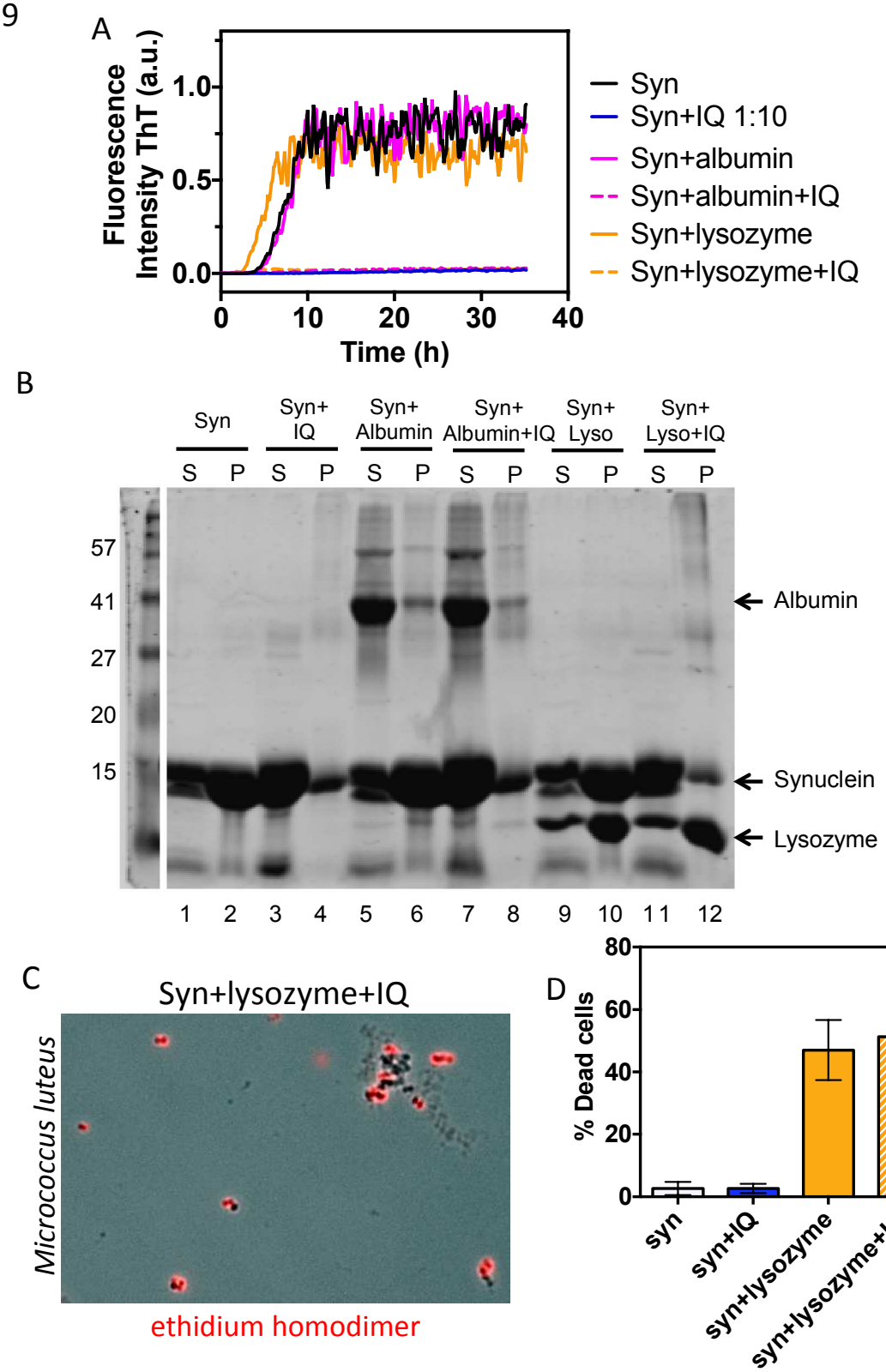
A
Fluorescence Intensity ThT (a.u.)
1.0
0.5
0.0
0
10
20
30
40
Time (h)
Syn
Syn+IQ 1:10
Syn+albumin
Syn+albumin+IQ
Syn+lysozyme
Syn+lysozyme+IQ
B
Syn
Syn+ IQ
Syn+ Albumin
Syn+ Albumin+IQ
Syn+ Lyso
Syn+ Lyso+IQ
S P S P S P S P S P S P
57
41
27
20
15
Albumin
Synuclein
Lysozyme
1 2 3 4 5 6 7 8 9 10 11 12
C
Syn+lysozyme+IQ
Micrococcus luteus
ethidium homodimer
D
% Dead cells
80
60
40
20
0
syn
syn+IQ
syn+lysozyme
syn+lysozyme+IQ

2

Table of Contents (TOC)